*J. Synchrotron Rad.* (1998). **5**, 729–731

# A soft X-ray (80–1500 eV) grazing-incidence monochromator with varied-line-spacing plane gratings at PF-BL-11A

**Yoshinori Kitajima,[a]* Kenta Amemiya,[b] Yoshiki Yonamoto,[b] Toshiaki Ohta,[b] Takashi Kikuchi,[a] Takashi Kosuge,[a] Akio Toyoshima[a] and Kenji Ito[a]**

*[a]Photon Factory, Institute of Materials Structure Science, High Energy Accelerator Research Organization, Oho 1-1, Tsukuba, Ibaraki 305-0801, Japan, and [b]Department of Chemistry, Graduate School of Science, The University of Tokyo, Hongo 7-3-1, Bunkyo, Tokyo 113-0033, Japan. E-mail: yoshinori.kitajima@kek.jp*

(*Received 4 August 1997; accepted 24 December 1997*)

The design and performance of a new soft X-ray beamline BL-11A at the Photon Factory (PF) are presented. A Hettrick-type grazing-incidence monochromator equipped with three varied-line-spacing plane gratings was designed and constructed at a bending-magnet source of the PF 2.5 GeV storage ring. An 800 lines mm$^{-1}$ laminar grating produced by aspheric-wavefront holographic recording optics, as well as a mechanically ruled blazed one, were tested. A resolving power of more than 4500 was achieved at 400 eV with either grating, and $\sim 10^{10}$ photons s$^{-1}$ are available at a resolving power of 2000. High photon flux enables low-concentration samples, such as surface adsorbates, to be studied. A simple scanning mechanism for a wide energy range is quite useful for EXAFS measurements on light elements such as C, N and O.

**Keywords: grazing-incidence monochromators; varied line spacing; holographic gratings; soft X-rays; EXAFS on light elements.**

## 1. Design of the new PF-BL-11A

In accordance with the upgrade of the PF 2.5 GeV storage ring to reduce the beam emittance, a beamline for soft X-ray spectroscopy (BL-11A) was to be reconstructed. Design concepts are as follows:

(i) Coverage of at least the same energy range (80–1000 eV) as the previous monochromator (Grasshopper Mark VII) at BL-11A;

(ii) Greatly improved achievable resolving power and available photon flux;

(iii) Stable scanning over a wide energy range for EXAFS measurements on light elements such as C, N and O, since the light source is not an undulator but a normal bending magnet (BM);

(iv) Variable-polarization capability by accepting a vertical portion of the BM radiation.

To meet these concepts, we adopted a Hettrick-type grazing-incidence monochromator with varied-line-spacing (VLS) plane gratings (Hettrick & Bowyer, 1983; Hettrick *et al.*, 1988), which had already been successfully constructed at ALS (Underwood *et al.*, 1997). The design procedure for the optical systems including the grating parameters has been described elsewhere in detail (Amemiya *et al.*, 1996, 1997).

The layout of the new beamline PF-BL-11A is shown schematically in Fig. 1. A vertical aperture (S0) is defined by two independent directly water-cooled Cu blocks. They are inserted from the top and bottom sides with stepping motors to pass the beam centred for linear polarization or off-centred for circular polarization. This aperture is also useful in the search for the vertical focusing position (Amemiya *et al.*, 1997). Synchrotron radiation is deflected and partly focused horizontally by a cylindrical mirror (M0), and then focused vertically by another cylindrical mirror (M0′) to the water-cooled entrance slit (S1), with its opening variable from 2 μm to 5 mm. A V-shaped aperture and a fluorescent screen monitor were set upstream and downstream of S1, respectively. The whole system of the slit including the vacuum chamber can be translated along the beam by ±20 mm. To cover a wide energy range, two spherical mirrors (M1 and M2) are prepared for different included angles, and M1 can be removed from the light path with a linear translation mechanism when M2 is used. The whole mechanism including the vacuum chamber for M1 and M2 can be translated along the beam to compensate for possible errors in the radii of the spherical mirrors by changing their pitching angles. Three varied-line-spacing plane gratings (VLS-PG) with different groove densities (300, 800 and 1200 lines mm$^{-1}$ are planned) are interchangeable by a linear-translation mechanism without breaking the vacuum. Grating rotation for scanning wavelength (±4° over the whole range) is performed with a sine-arm mechanism driven

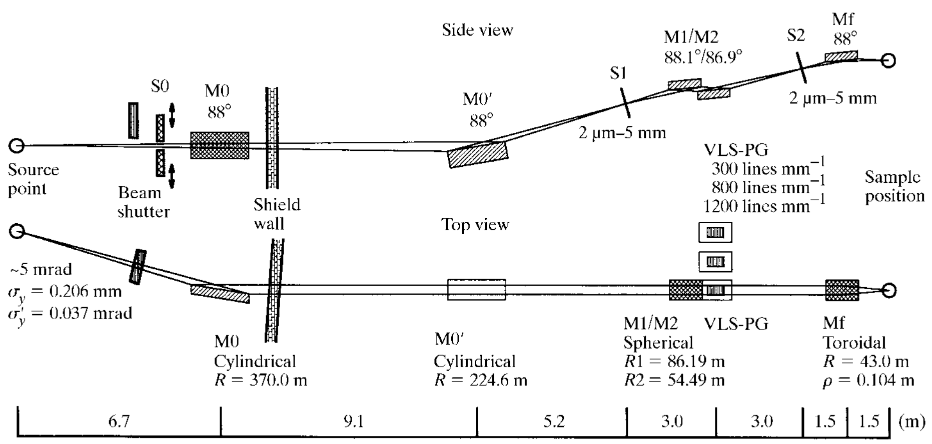


**Figure 1**
Schematic layout of the new beamline at PF-BL-11A.

by a stepping motor, and its position is monitored with a linear encoder. Pitching, rolling and yawing of each grating are also adjustable in the vacuum. The exit slit (S2) has the same mechanisms as S1 without water cooling. The monochromated beam thus obtained is refocused to the sample position by the toroidal mirror (Mf).

## 2. Initial performance of the new PF-BL-11A

### 2.1. *Mechanically ruled 800 lines mm$^{-1}$ grating*

An 800 lines mm$^{-1}$ blazed grating produced by the mechanical ruling method (Hitachi Corporation) was tested firstly. Fig. 2(*a*) shows the photoion spectrum of $N_2$ gas with this grating and M2. The estimated resolving power, $E/\Delta E$, is 6900 at 401 eV, indicating that the grating parameters are well controlled and alignment of the beamline components is successful. Here we used the value of 117 meV as the natural lifetime width for N 1*s* $\rightarrow$ $\pi$* resonance in $N_2$ (Watanabe *et al.*, 1997). This combination of the 800 lines mm$^{-1}$ grating and M2 covers the energy range from 200 eV to higher than 1000 eV, as shown in Fig. 3(*a*).

### 2.2. *Holographically recorded 800 lines mm$^{-1}$ grating*

A laminar grating, having almost the same groove parameters as the mechanically ruled one, was produced by the aspheric wavefront holographic recording technique (Shimadzu Corporation) and tested (Amemiya *et al.*, 1997). The $N_2$ 1s $\rightarrow$ $\pi$* spectrum shown in Fig. 2(*b*) clearly demonstrates that the quality of the grating is sufficiently high, although the ultimate resolving power ($\sim$4500) is slightly lower than that of the mechanically ruled grating. Fig. 3(*b*) shows the spectral distribution with the holographic grating and M2, which was measured by the photoemission current from a gold-coated tungsten mesh. Due to the benefit of the smooth surface of the holographic grating, scattered light is effectively suppressed compared with that from a mechanically ruled grating.

### 2.3. *Lower and higher energy regions*

Although a sufficient 300 lines mm$^{-1}$ grating (mechanically ruled) has not been satisfactorily commissioned yet, it was confirmed that photons with an energy down to 80 eV are obtainable, as shown in Fig. 3(*c*). We have not yet obtained a 1200 lines mm$^{-1}$ grating but the combination of the 800 lines mm$^{-1}$ grating and M1 can be used for the higher-energy region, as shown in Fig. 3(*d*).

### 2.4. *Photon flux versus resolving power*

Although a high resolving power can be obtained as described above, the photon flux (*e.g.* $\sim$10$^8$ photons s$^{-1}$ with $E/\Delta E$ = 5000 at a photon energy of 400 eV) is much lower compared with that of the undulator beamlines (Shigemasa *et al.*, 1998; Watanabe *et al.*, 1997) under such conditions. At the sacrifice of the resolution, we can obtain higher photon fluxes: $\sim$10$^{10}$ photons s$^{-1}$ with $E/\Delta E$ = 2000 and $\sim$10$^{11}$ photons s$^{-1}$ with $E/\Delta E$ = 600 at a photon energy of 400 eV. It is more than 5–50 times that of the former Grasshopper monochromator.

### 2.5. *Linear polarization factor and higher-order diffraction*

The linear polarization factor was estimated to be 0.955 from the photofragment ion yield ratio between parallel and perpendicular detection for the $N_2$ 1*s* $\rightarrow$ $\pi$* transition. Higher-order light is not negligible, especially with the holographic grating. For example, at $\sim$250 eV, $\sim$10% in intensity of the second-order light ($\sim$500 eV) and $\sim$10% of third-order light ($\sim$750 eV) are mixed. A double mirror set for higher-order suppression is now under construction.

### 2.6. *EXAFS spectra measurements*

As a first example of surface EXAFS measurements on light elements at this beamline, the oxygen *K*-edge spectra were measured for submonolayer-adsorbed methoxy ($CH_3O-$) species on Ni(111) by partial electron yield detection. The spectra of adsorbates were divided by those of clean Ni. Fig. 4 shows a spectrum at normal incidence, in which the accumulation time was 90 s per point for the $CH_3O$-adsorbed sample and 20 s per point for clean Ni(111). A total measurement time of $\sim$8 h is tolerable for studying adsorption structure.

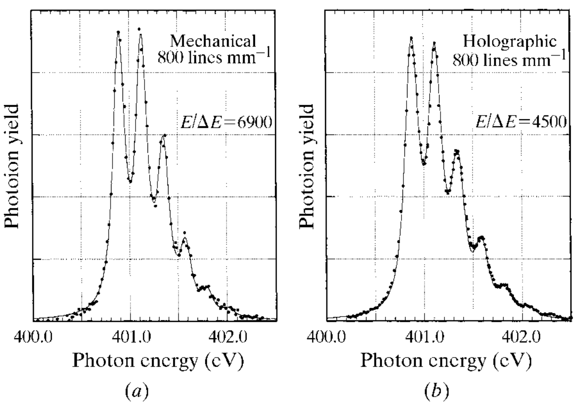


**Figure 2**
Photoion spectra of $N_2$ gas measured with (*a*) a mechanically ruled 800 lines mm$^{-1}$ grating and (*b*) a holographically recorded 800 lines mm$^{-1}$ grating.

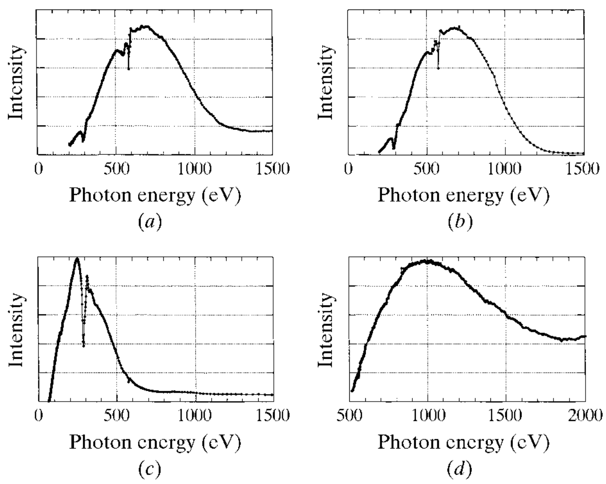


**Figure 3**
Transmission curves with the combinations of (*a*) the mechanically ruled 800 lines mm$^{-1}$ grating and M2, (*b*) the holographically recorded 800 lines mm$^{-1}$ grating and M2, (*c*) the mechanically ruled 300 lines mm$^{-1}$ grating and M2, and (*d*) the mechanically ruled 800 lines mm$^{-1}$ grating and M1. All the spectra were measured by the photoemission current from a gold-coated tungsten mesh.

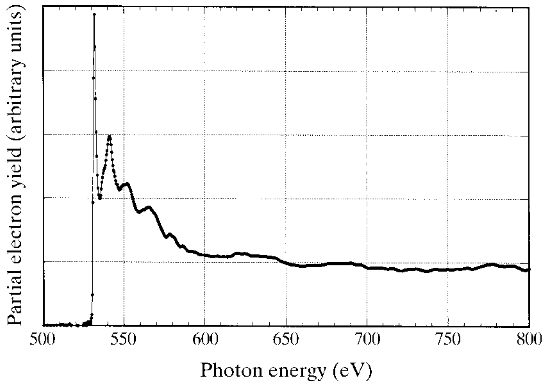


**Figure 4**
Oxygen *K*-edge EXAFS spectrum for submonolayer-adsorbed methoxy ($CH_3O-$) species on Ni(111).

The authors would like to express sincere thanks to the following individuals and groups for their kind suggestions, comments and/or cooperation for designing, construction and commissioning of the beamline and grating: Dr Masato Koike (LBL, JAERI), Dr Shoji Suzuki (Tohoku University), Dr Eiji Ishiguro (Osaka City University, Ryukyu University), Dr Tetsuji Sekitani (PF, Hiroshima University), Dr Atsunari Hiraya (IMS, Hiroshima University), Dr Hiromichi Shimada (NIMC), Dr Tatsuji Hayaishi (University of Tsukuba), Dr Toshiaki Kita (Hitachi Co. Ltd), Dr Kazuo Sano (Shimadzu Co. Ltd), Professor Kazuhiko Seki's group (Nagoya University) and Professor Nobuhiro Kosugi's group (IMS).

## References

Amemiya, K., Kitajima, Y., Ohta, T. & Ito, K. (1996). *J. Synchrotron Rad.* **3**, 282–288.

Amemiya, K., Kitajima, Y., Yonamoto, Y., Ohta, T., Ito, K., Sano, K., Nagano, T., Koeda, M., Sasai, H. & Harada, Y. (1997). *Proc. SPIE*, **3150**, 171–182.

Hettrick, M. C. & Bowyer, S. (1983). *Appl. Opt.* **22**, 3921–3924.

Hettrick, M. C., Underwood, J. H., Batson, P. J. & Eckart, M. J. (1988). *Appl. Opt.* **27**, 200–202.

Shigemasa, E., Toyoshima, A., Yan, Y., Hayaishi, T., Soejima, K., Kiyokura, T. & Yagishita, A. (1998). *J. Synchrotron Rad.* **5**, 777–779.

Underwood, J. H., Gullikson, E. M., Koike, M. & Batson, P. J. (1997). *Proc. SPIE*, **3113**, 214–221.

Watanabe, M., Toyoshima, A., Azuma, Y., Hayaishi, T., Yan, Y. & Yagishita, A. (1997). *Proc. SPIE*, **3150**, 58–66.